JCB Article

Sinuous is a *Drosophila* claudin required for septate junction organization and epithelial tube size control

Victoria M. Wu,[1] Joost Schulte,[2] Alexander Hirschi,[1] Ulrich Tepass,[2] and Greg J. Beitel[1]

[1]Department of Biochemistry, Molecular Biology, and Cell Biology, Northwestern University, Evanston, IL 60208
[2]Department of Zoology, University of Toronto, Toronto, Ontario M5S 3G5, Canada

Epithelial tubes of the correct size and shape are vital for the function of the lungs, kidneys, and vascular system, yet little is known about epithelial tube size regulation. Mutations in the *Drosophila* gene *sinuous* have previously been shown to cause tracheal tubes to be elongated and have diameter increases. Our genetic analysis using a *sinuous* null mutation suggests that *sinuous* functions in the same pathway as the septate junction genes *neurexin* and *scribble*, but that *nervana 2*, *convoluted*, *varicose*, and *cystic* have functions not shared by *sinuous*. Our molecular analyses reveal that *sinuous* encodes a claudin that localizes to septate junctions and is required for septate junction organization and paracellular barrier function. These results provide important evidence that the paracellular barriers formed by arthropod septate junctions and vertebrate tight junctions have a common molecular basis despite their otherwise different molecular compositions, morphologies, and subcellular localizations.

Introduction

Major organs such as the lung, vascular system, and kidney are composed of endothelial and epithelial tubes that have reproducible sizes and shapes. Tubes that deviate from their normal sizes can cause medical conditions such as polycystic kidney disease and ischemia. However, the cell biological and molecular mechanisms by which cells assemble into tubes with highly regulated lengths and diameters is poorly understood. The *Drosophila* tracheal system provides a genetically tractable model system to investigate the molecular processes of tubulogenesis (for review see Manning and Krasnow, 1993). The tracheal system is a network of ramifying epithelial tubes that forms the gas exchange organ of the fly, but it also functions analogously to the vertebrate vascular system by delivering oxygen directly to the tissues. The tracheal system is created from 20 clusters of ~80 epithelial cells each that undergo a series of coordinated movements and junctional rearrangements to produce a complex network of tubes (Fig. 1 A). These tubes have characteristic diameters and lengths that undergo developmentally regulated size changes (Beitel and Krasnow, 2000).

In a genetic screen to identify genes that are required for epithelial tube size control, we isolated mutations in *sinuous* (*sinu*) and seven other genes that cause defects in a specific increase in tracheal diameter that occurs over an ~2-h period late in embryogenesis (Beitel and Krasnow, 2000). Embryos homozygous for mutations in these genes have normal trachea before this "tube expansion," but during tube expansion, the lengths and diameters of multicellular tracheal tubes become abnormally increased, resulting in tracheal tubes that follow tortuous pathways and have local diameter expansions. As the number of tracheal cells in these mutants is not increased, the increased tube sizes must result from changes in cell shape (Beitel and Krasnow, 2000). Recently, we cloned one of these genes, *nervana 2* (*nrv2*), and found that it encodes a Na/K ATPase β-subunit that is a component of pleated septate junctions (Paul et al., 2003). Further, we found that the septate junction proteins Neurexin (Nrx) and Coracle (Cor), which are homologous to the vertebrate CASPR and band 4.1 proteins, respectively, are also required for tracheal tube expansion (Paul et al., 2003). In this report, we show that Sinuous encodes a claudin that plays a critical role in septate junction function.

The best-characterized function of invertebrate pleated septate junctions, hereafter referred to simply as septate junctions, is to form a barrier that prevents free diffusion of water and solutes between adjacent epithelial cells (for review

The online version of this article includes supplemental material.

Address correspondence to Greg Beitel, Department of Biochemistry, Molecular Biology, and Cell Biology, Northwestern University, Hogan Hall, Rm. 2-100, Northwestern University, 2205 Tech Drive, Evanston, IL 60208-3500. Tel.: (847) 467-7776. Fax: (847) 467-1380. email: beitel@northwestern.edu

Key words: tight junction; *Drosophila*; epithelial cell; trachea; morphogenesis

Abbreviations used in this paper: Arm, Armadillo; *conv*, *convoluted*; Cor, coracle; Dlg, Discs large; Dlt, Discs lost; FasIII, Fasciclin III; Mega, megatrachea; Nrv2, nervana 2; Nrx, neurexin; *scrib*, *scribble*; TEM, transmission electron microscopy; *vari*, *varicose*.

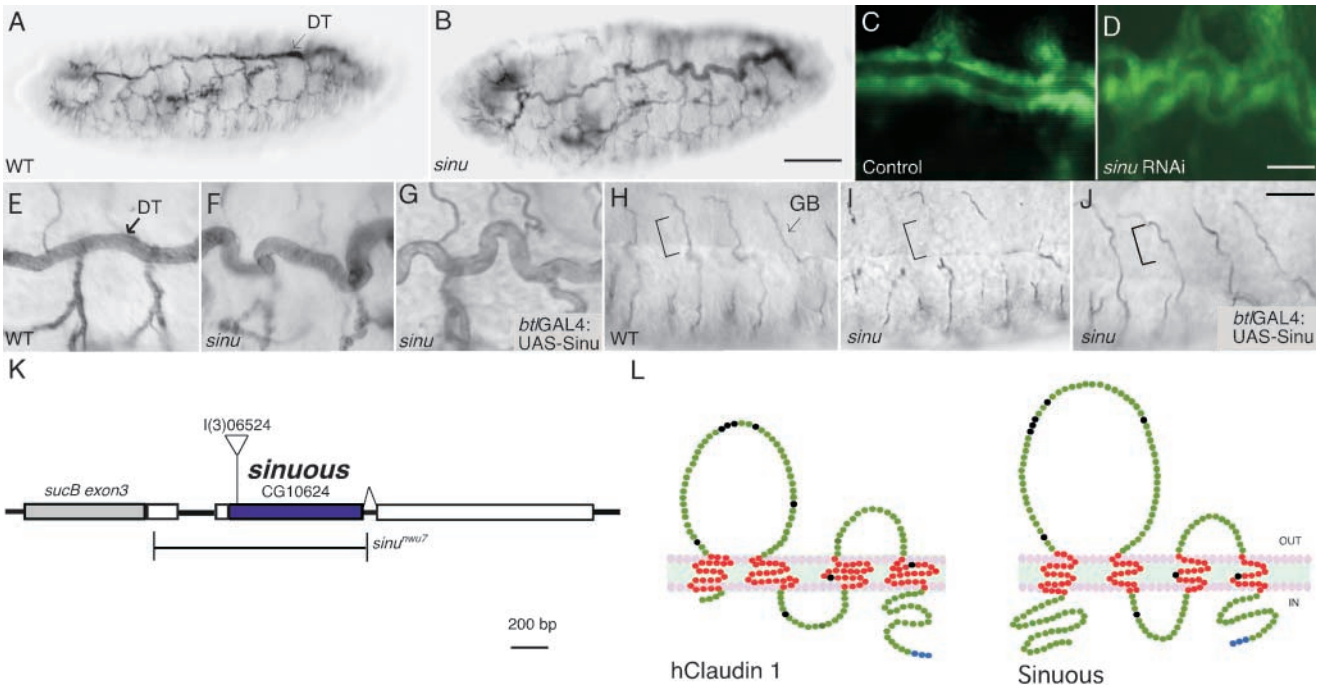

Figure 1. **Sinuous encodes a claudin family member required for tracheal tube size control.** (A–G) The multicellular tracheal dorsal trunks (DT) in *sinuous* mutants (B and F) have trachea that are too long and have some diameter expansions compared with wild-type (WT) animals (A and E). (H–J) *sinuous* mutants (I) also have missing lumenal segments in their ganglionic branches (GB), where tubes are formed by single cells with autocellular junctions (square brackets). (C and D) Injection of double-stranded RNA corresponding to *CG10624* into *btl*-GAL4:UAS-GFP embryos causes the same phenotypes as *sinuous* mutants (D), whereas buffer-injected control embryos have normal trachea (C). Expression of the CG10624 ORF in *sinuous* homozygotes using the *btl*-GAL4 tracheal driver and a UAS-Sinuous responder rescues the ganglionic branch defects (J), but not the dorsal trunk length defects (G). *btl*-GAL4 driven expression of Sinuous in the tracheal system in an otherwise WT background did not cause any apparent defects (not depicted). (K) A schematic representation of the *sinuous* locus. The *sinuous*$^{l(3)06524}$ strain contains a transposable element insertion at the beginning of the CG10624 ORF. *sinu*^{nwu7} is a null mutation that deletes all the amino acids of the *sinuous* ORF without affecting the coding sequences of adjacent genes. (L) Sinuous is predicted to encode a 247-aa protein with four transmembrane domains and a topology similar to vertebrate claudins. hClaudin-1 is shown as a representative vertebrate claudin. Conserved claudin residues present in Sinuous and hClaudin-1 are shown in black, and the putative PDZ-binding domain residues are blue (see Results for details). Predicted transmembrane domain residues are red. All embryos stage 16; A, B, and E–J stained with the anti-lumenal 2A12 mAb. Genotypes: wild-type, Oregon-R; *sinu*^{nwu7}; *sinuous* rescue, *blt*-GAL4 UAS-Sinuous; *sinu*^{nwu7}. Bars: B, 50 μm (for A and B); D, 10 μm (for C

see Tepass et al., 2001). The paracellular barrier in vertebrates is formed by tight junctions (for review see Anderson, 2001; Tsukita et al., 2001); however, septate and tight junctions have been considered analogous rather than homologous structures because of the dramatic morphological and molecular differences between them. Tight junctions lie apically to adherens junctions and have "kissing points" where the intercellular space is periodically obliterated (Farquhar and Palade, 1963; Staehelin, 1974; Schneeberger and Lynch, 1992; Tsukita et al., 2001). On the other hand, septate junctions lie basally to adherens junctions and have regularly spaced septa bridging an ~15-nm intercellular space (Lane and Swales, 1982; Tepass et al., 2001). Both tight and septate junctions form continuous barriers around cells, but tight junctions appear as a network of anatomizing strands of particles, whereas arthropod septate junctions appear as ribbons that are tightly parallel to each other (Claude and Goodenough, 1973; Lane and Swales, 1982). In addition to barrier function, tight junctions also have a "fence" function that is thought to create a boundary between apical and basolateral domains (Schneeberger and Lynch, 1992; Tsukita et al., 2001). Although possible fence functions of septate junctions have not been investigated in detail, mutations that compromise septate junction components such as Cor, Nrx or the Na/K ATPase do not cause mislocalization of apical epithelial markers (Baumgartner et al., 1996; Lamb et al., 1998; Genova and Fehon, 2003; Paul et al., 2003).

At the molecular level, many *Drosophila* homologues of vertebrate tight junction proteins including DaPKC/aPKC, DmPar6/ASIP, Crumbs/CRB1, and polychaetoid/ZO 1-3 do not localize to the septate junction, but instead are found in the adherens junction or the marginal zone, which, like the tight junction, lies apically to the adherens junction (for review see Tepass et al., 2001; Knust and Bossinger, 2002). Furthermore, the *Drosophila* genome appears to lack the tight junction proteins occludin and junction adhesion molecule (Tepass et al., 2001; unpublished data), and claudins were reported to be absent from the *Drosophila* genome (Kollmar et al., 2001).

Vertebrate claudins are highly divergent, four-transmembrane domain proteins that homo- and heterophilically interact to form the paracellular barrier in the tight junctions (Tsukita et al., 2001; Tsukita and Furuse, 2002). Claudins were first identified by Furuse et al. (1998) and were subsequently shown to be a large multigene family (Morita et al., 1999) that currently has at least 19 human members (Koll-

mar et al., 2001). When expressed in nonadherent cells, several vertebrate claudins can mediate homophilic cell–cell adhesion and assemble strands reminiscent of those found at tight junction kissing points (Furuse et al., 1998; Kubota et al., 1999). Evidence that claudins directly form the paracellular barrier comes from the demonstrations that mice lacking claudin-1 or -5 display apparently normal tight junction ultrastructure, but show altered paracellular permeability (Furuse et al., 2002; Nitta et al., 2003). In addition, amino acids in the first extracellular loop of claudins determine the charge selectivity and resistance of tight junctions (Colegio et al., 2002, 2003). Together, the divergent morphologies of septate and tight junctions, coupled with the apparent absence of claudins in *Drosophila* septate junctions, has supported the view that the epithelial barrier junctions in insects and vertebrates are analogous rather than homologous structures.

Here, we provide critical evidence that the paracellular barriers of septate and tight junctions have a common molecular basis. Sinuous is predicted to have the same membrane topology as vertebrate claudins, and has molecular similarity to canonical vertebrate claudins comparable to that of several more divergent vertebrate claudins. Furthermore, Sinuous localizes to *Drosophila* paracellular barrier junctions and is required for barrier function. Thus, Sinuous has both molecular and functional similarities to vertebrate claudins. In investigating the relationship between Sinuous and other septate junction components, we determined that the localization of Sinuous to septate junctions depends on other septate junction components including Nrx, Cor, Megatrachea (Mega), and Nrv2. Further, we found that *sinuous* appears to function in the same genetic pathway of septate junction–mediated tracheal tube size control as *nrx* and the cell polarity/septate junction gene *scribble* (*scrib*), but that the *nrv2* Na/K ATPase β-subunit and the as-yet-uncloned genes *convoluted* (*conv*), *varicose* (*vari*), and *cystic* have tube size control functions not shared by *sinuous*.

Results

Sinuous encodes a claudin family member

To begin to understand the role of *sinuous* in tracheal tube size control, we cloned and characterized the *sinuous* gene. Using inverse PCR, we determined that the transposable element in the $sinuous^{l(3)06524}$ strain had inserted into the beginning of the ORF of predicted gene *CG10624* (Fig. 1 K). Transposon mobilization experiments showed that the insertion in the *l(3)06524* line caused the *sinuous* phenotype (Fig. 1, B, F, and I), as only precise excisions produced homozygous viable embryos with wild-type trachea (unpublished data). We confirmed that disruption of the *CG10624* transcript caused the tracheal phenotypes by showing that RNA interference knockdown of *CG10624* phenocopied the tracheal defects of $sinuous^{l(3)06524}$ mutants (Fig. 1 D), and that expression of a *CG10624* cDNA under the control of a tracheal driver partially rescued the tracheal defects of *sinuous* mutants (Fig. 1, G and J). Together, these results demonstrate that *CG10624* is *sinuous*.

Based on the sequences of 11 cDNAs and the PCR products of 5′ RACE experiments, *sinuous* is predicted to encode a single isoform of a 247-aa protein (see Materials and methods). The Pfam algorithm (Bateman et al., 2002) identifies Sinuous as a member of the claudin/PMP-22/EMP protein family, and the TMHMM transmembrane algorithm (Sonnhammer et al., 1998) predicts Sinuous to have a topology characteristic of claudins—four transmembrane domains, intracellular NH_2 and COOH termini, a larger first extracellular loop, and two smaller loops (Fig. 1 L). As with almost all vertebrate claudins, Sinuous has a PDZ domain–binding site at its COOH terminus.

Table I. **Number of conserved amino acids in claudin family members**

Gene	Conserved residues (x/13)[a]
hClaudin-1	13
hClaudin-11	12
hClaudin-10	11
hClaudin-12	9
Sinuous	**9**
fly CG1298	9
fly CG6398	7
fly CG3770	7
fly CG14779	7
fly CG6982	6
ceCLC-3	8
ceCLC-4	8
ceCLC-1	6
ceCLC-2	4
ceVAB-9	5
dog TM4SF10	5

h, human; ce, *C. elegans*.
[a]Number of the 13 amino acids that are conserved among 90% of chordate claudins (Fig. S1, available at http://www.jcb.org/cgi/content/full/jcb.200309134/DC1).

To assess the similarity between Sinuous and other claudin family members, we compared Sinuous with the chordate claudins analyzed by Kollmar et al. (2001), the recently identified *Caenorhabditis elegans* claudins and claudin-like proteins CLC-1 through CLC-4 (Asano et al., 2003) and VAB-9 (Simske et al., 2003), and five other *Drosophila* claudin family members that we and others have identified (Tepass et al., 2001; Behr et al., 2003; Table I and Fig. S1, available at http://www.jcb.org/cgi/content/full/jcb.200309134/DC1). Sinuous has ∼20% sequence identity and 36% similarity with human claudins, which is comparable to the <25% identity and 40% similarity between more divergent members of the human claudins. More informatively, Sinuous has 9 of the 13 residues conserved among 90% of the 36 chordate claudins characterized by Kollmar et al. (2001) (Table I; Fig. S1). In comparison, human claudin-12 and claudin-10 have 9 and 11 of these 13 residues; *Drosophila* Mega, CG3770, and CG6398 each have 7 or less of the 13; and the *C. elegans* CLC-1 through CLC-4 have between four and eight of these conserved residues (Table I). Together, these observations indicate that Sinuous is a claudin and contains more residues characteristic of claudins than most *C. elegans* or *Drosophila* claudins.

To investigate the evolutionary relationship between invertebrate and vertebrate claudins, we aligned the sequences of a set of claudin family proteins (Fig. S1, available at http://www.jcb.org/cgi/content/full/jcb.200309134/DC1; see Materials and methods) and constructed a phylogenetic tree us-

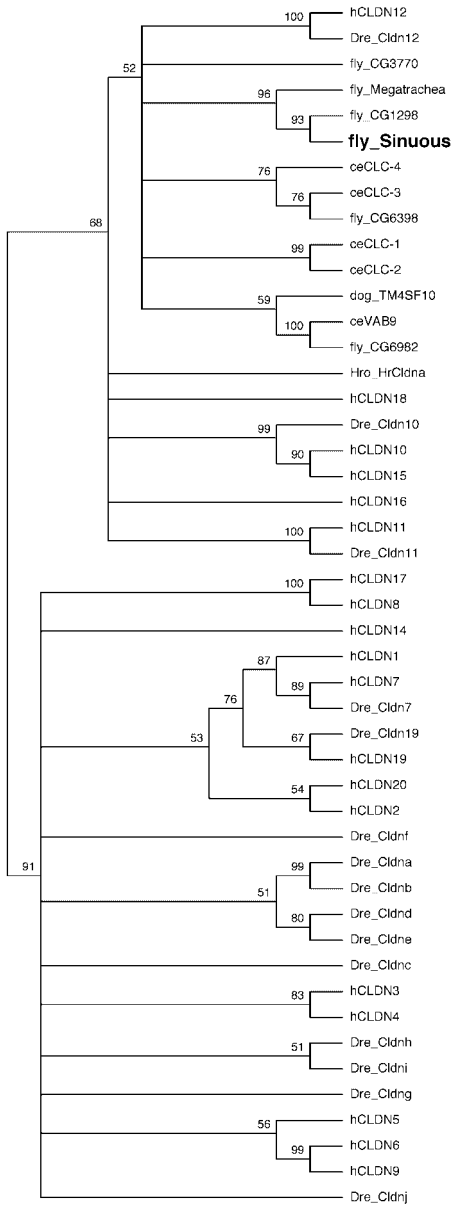

Figure 2. **Invertebrate and vertebrate claudins form a highly divergent protein family.** The phylogenetic tree resulting from a bootstrap analysis of aligned claudin family member sequences (Fig. S1, available at http://www.jcb.org/cgi/content/full/jcb.200309134/DC1; see Materials and methods). Numbers indicate the frequency with which particular nodes occurred among individual trees generated from 1,000 random samplings of the aligned sequences. Unlabeled nodes occurred in <51% of individual trees. Dog TM4SF10 is also known as BCMP-1 (Christophe-Hobertus et al., 2001). fly, *D. melanogaster*; Dre, zebra fish; ce, *C. elegans*; Hro, *Halocynthia roretzi*.

ing a bootstrap approach that more robustly determines relationships between proteins with limited sequence conservation than do "best-fit" tree approaches (Fig. 2). Although several of the zebrafish and human claudins cluster together, 10 of the 15 zebrafish claudins do not (Kollmar et al., 2001). Similarly, neither Sinuous nor other invertebrate claudins closely cluster with particular vertebrate claudins, but they do fall in a subgroup that includes human claudin-12 (Fig. 2), which has been implicated in formation of the tight junctions of endothelial cells that constitute the blood–brain barrier (Nitta et al., 2003). Sinuous is most closely related to *Drosophila* CG1298, but even CG1298 is only 35% identical and 56% similar to Sinuous. Thus, *Drosophila* claudins show the same remarkable sequence divergence as claudins in other species, and this divergence obscures identification of possible Sinuous orthologues.

Sinuous localizes to septate junctions

If Sinuous were to act similarly to vertebrate claudins in forming the paracellular diffusion barrier, we would expect Sinuous to localize to septate junctions rather than to the more apical marginal zone where many *Drosophila* homologues of vertebrate tight junction proteins localize. As assessed by immunohistochemistry, Sinuous begins to be expressed in ectodermally derived tissues at stage 13, and predominantly colocalizes with Cor at the septate junction when it becomes discernible by confocal microscopy at late stage 13 (Fig. S2, available at http://www.jcb.org/cgi/content/full/jcb.200309134/DC1). From stage 15 onwards, Sinuous colocalizes with Cor and Nrx at septate junctions, although some diffuse staining that extends more basally than Cor staining is also visible (Fig. 3, A–C′′; Fig. S2). Sinuous localizes basally to the adherens junction markers Armadillo (β-catenin/Arm) and DE-cadherin (Fig. 3, D–D′′; unpublished data). Together, these results show that Sinuous is a component of septate junctions.

Sinuous is required for septate junction organization and barrier function

We determined whether Sinuous was required for paracellular barrier function using the assay of Lamb et al. (1998), which tests the ability of the tracheal and salivary gland epithelia to exclude a 10-kD dye that has been injected into the body cavity of an embryo (see Materials and methods). For these and subsequent experiments, we used the *sinuous* null mutation $sinu^{nwu7}$, which deletes all of the Sinuous coding sequence without affecting the coding sequence of adjacent genes (Fig. 1 K; see Materials and methods). In *sinuous* mutants, paracellular barrier function is compromised and the dye freely enters the tracheal and salivary gland lumens in all animals examined (Fig. 4 D; unpublished data; $n = 18$ for salivary glands, 26 for trachea). Thus, Sinuous localizes to septate junctions and is required for their paracellular barrier function.

To investigate the molecular basis of the barrier defects in *sinuous* mutants, we determined the subcellular localization of septate junction markers Cor, Nrx, ATPα, Discs large (Dlg), and Fasciclin III (FasIII) in *sinuous* null mutants. We examined four distinct ectodermally derived tissues to assess possible tissue specificity and to better visualize Sinuous' subcellular localization. The hindgut and salivary glands are columnar epithelia in which the subcellular localization of septate junction markers is more obvious, as septate junctions are restricted to the apical third of the lateral membrane (Fig. 4, A and A′′′). In contrast, the tracheal cells are squamous, and assessment of subcellular localization is more difficult because septate junctions occupy most of the lateral membrane surfaces (Fig. 4 A′′; Tepass and Hartenstein, 1994). In the epidermis, hindgut and trachea of *sinuous* null mutants, Cor, Nrx, ATPα, and Dlg are mislocalized basally (Fig. 4, B–B′′) and/or have re-

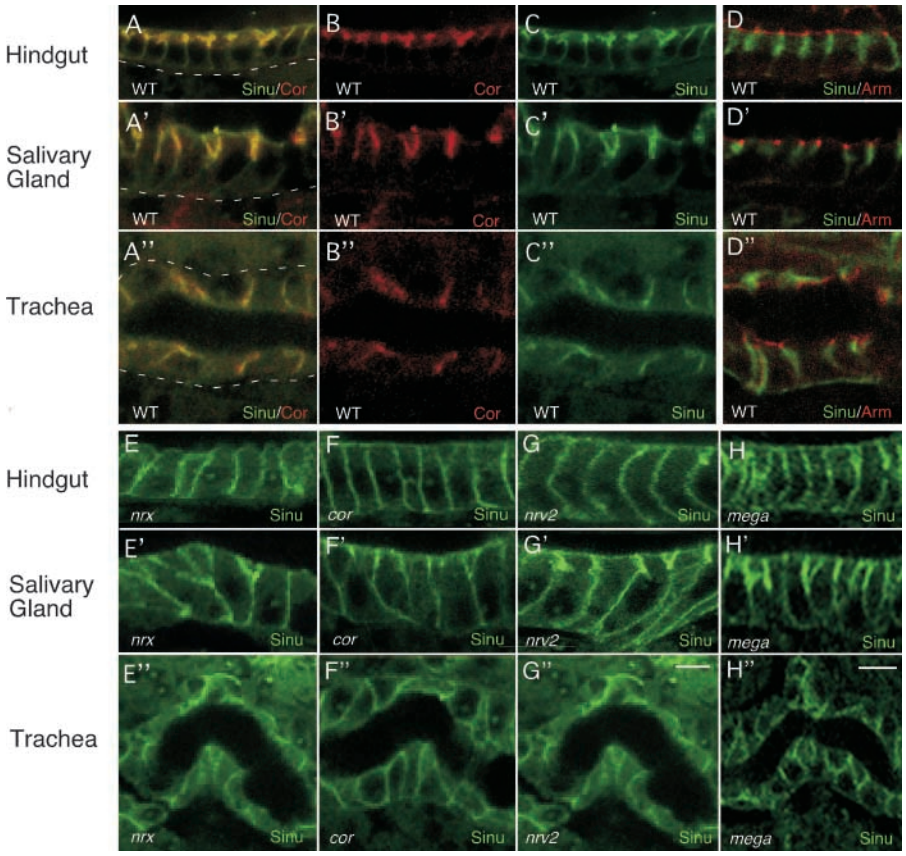

Figure 3. **Sinuous localizes to septate junctions in wild-type animals, but not in most septate junction mutants.** In wild-type embryos stained with anti-Sinuous (A and C, green) and anti-Cor (A and B, red) antibodies, Sinuous colocalizes almost entirely with Cor at septate junctions in the hindgut, salivary gland, and trachea (A–A′′). (D) Sinuous (green) does not localize to the adherens junctions, marked by Arm (D–D″; red). (E–H) Sinuous localization to septate junctions depends on Cor, Nrx, Mega, and Nrv2 as Sinuous is mislocalized and/or reduced in animals homozygous for null mutations in these genes (E–H″). In the partial loss-of-function $mega^{VE896}$ mutants, the localization and levels of Sinuous are reduced in the hindgut and trachea, but appear normal in the salivary glands (not depicted). All images of stage 16 animals. Dashed lines mark basal cell surfaces. Genotypes: WT, *sinu*/+; nrx^{4865}; cor^{5}; $nrv2^{23B}$; $sinu^{nwu7}$; $mega^{G0044}$. Bar in G and H (represents all panels), 5 μm.

duced levels (Fig. 4, F and F′). Surprisingly, despite the paracellular barrier defects of salivary glands in *sinuous* mutants (Fig. 4 D), the localization and approximate levels of Cor, Nrx, ATPα, and Dlg appear normal in salivary glands (Fig. 4 B′′′, F′′, and H′′; unpublished data). However, the more basal distribution of FasIII in salivary glands of *sinuous* mutants indicates that Sinuous does have a role in localizing some septate junction components in the salivary glands (Fig. 4 J′′). These observations suggest that although other proteins, such as the *Drosophila* claudin Mega (Behr et al., 2003), can be sufficient for correct subcellular localization of many septate junction components in some tissues, Sinuous is required in all tissues for the correct function or organization of septate junctions at a level not resolved by confocal microscopy.

Sinuous does not appear to be required for adherens junction formation or overall apical/basal polarity, as the localizations and levels of the adherens junction markers Arm and the apical surface marker Discs lost (Dlt) appear normal in all tissues examined (Fig. 4, K–L′′). Together, these results show that Sinuous is required for septate junction organization and barrier function.

Sinuous mutants have a reduced number of septa and fragmented septate junction ribbons

To understand the role of Sinuous at the ultrastructural level, we examined septate junctions in *sinuous* mutants using transmission electron microscopy (TEM; Fig. 5). In wild-type embryos, septate junctions are composed of "ribbons" of proteinaceous material that run parallel to the apical cell surface in the plane of the membrane (Fristrom, 1982; Tepass and Hartenstein, 1994; Tepass et al., 2001; Schulte et al., 2003). These ribbons are believed to be the physical basis for the transepithelial diffusion barrier. Septate junctions contain many individual ribbons, most of which are clustered into closely stacked arrays. In TEM micrographs of late-stage wild-type embryos, ribbons appear as electron-dense septa that bridge the intercellular space, and the clustering is readily apparent (Fig. 5 A).

Despite the loss of paracellular barrier function in *sinuous* mutants, numerous, well-differentiated septa were visible in the trachea, epidermis, and salivary glands (Fig. 5, B and C; unpublished data). However, the total number of septa was significantly reduced, there were fewer groups of septa, and septa were not organized into continuous circumferential ribbons (Fig. 5 B). For example, in the epidermis of late stage 17 wild-type embryos, there were 16.0 ± 0.6 septa in 6.5 ± 0.3 groups ($n = 86$) per cell–cell contact. In contrast, *sinuous* mutants had 6.8 ± 0.8 septa ($P < 10^{-15}$) arranged in 3.3 ± 0.3 ($P < 10^{-11}$) groups ($n = 57$). The number of septa per cell–cell contact in *sinuous* mutants was highly variable, ranging from none to wild-type. Interestingly, in *sinuous* mutant salivary glands, although septal number was dramatically reduced from 66.5 ($n = 6$) to 16.2 ($n = 6$), the number of remaining septa was similar to that of wild-type epidermis, which may explain the near normal appearance of salivary gland septate junction markers by confocal microscopy (Fig. 4, B′′′, F′′, and H′′). However, there was also fragmentation of ribbons in the salivary glands because some cell–cell contacts displayed very few or no septa. Together, these findings demonstrate that although Sinuous is not es-

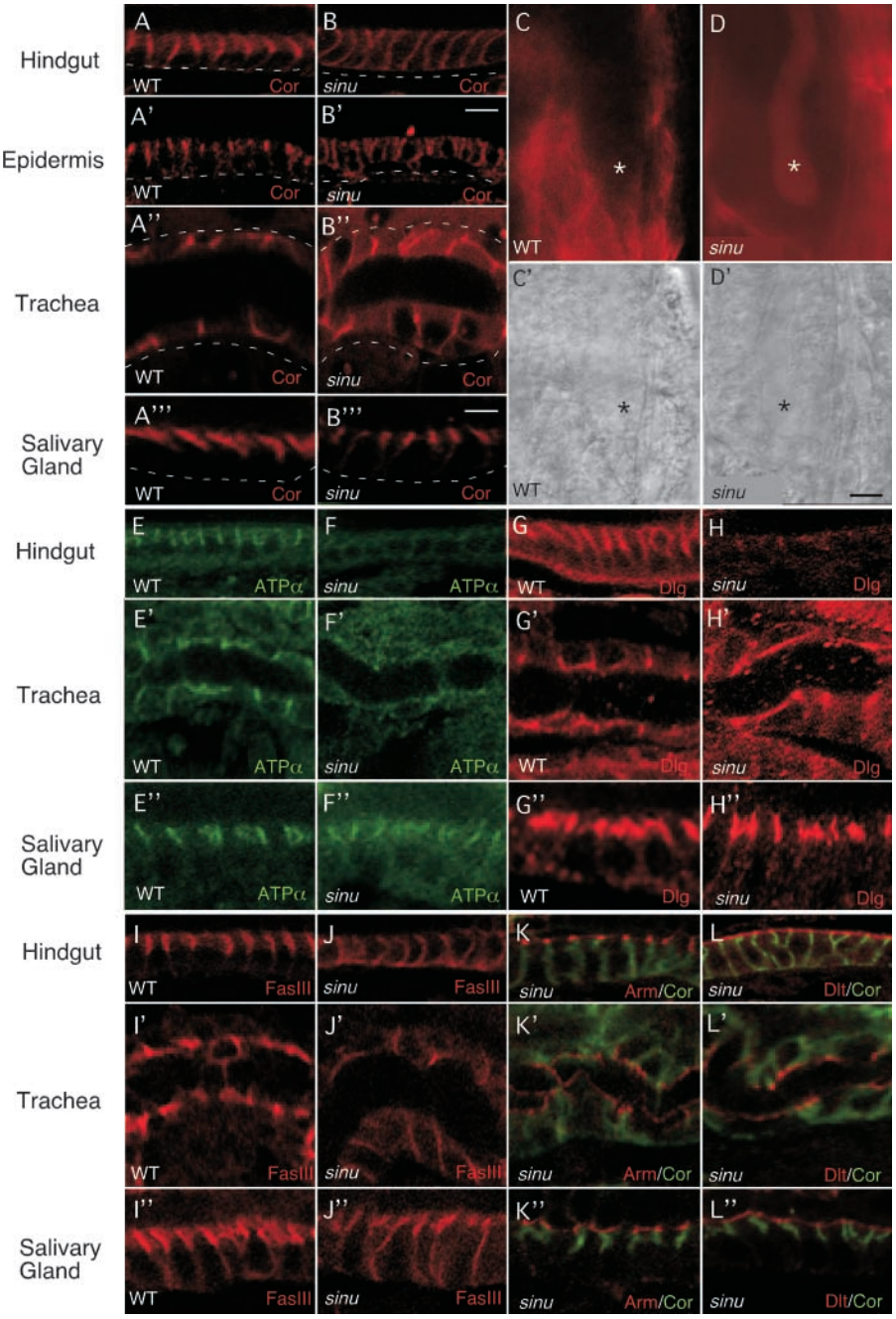

Figure 4. **Sinuous is required for septate junction organization and paracellular barrier function.** In *sinuous* mutants (B, D, F, H, and J–L), Cor (B–B′′′, red; K–L′′, green), the Na/K ATPase α-subunit (ATPα; F-F′′, green), Dlg (H–H′′, red,) and Nrx (not depicted) are mislocalized and/or reduced in the epidermis, hindgut, and trachea compared with wild-type animals (A–A′′, E–E′, G–G′, and I–I′). Surprisingly, the localization of these markers in *sinuous* mutant salivary glands appears normal (A′′′, F′′, H′′, and not depicted). In contrast, FasIII is only somewhat mislocalized/reduced in *sinuous* mutant salivary glands (J′′) and dramatically in mutant hindgut and trachea (J and J′). *sinuous* mutations specifically affect septate junctions, as the localization of the adherens junction component Arm (K–K′′) and the apical membrane marker Dlt (L–L′′) are unaffected in *sinuous* mutants. Basal surfaces are outlined with dashed white lines. (C–D′) The transepithelial diffusion barrier is compromised in *sinuous* mutants. A fluorescently labeled 10-kD dye injected into the body cavity does not cross the salivary gland epithelia in wild-type embryos (C, asterisk), but does in *sinuous* mutants (D, asterisk). (C′ and D′) Differential interference contrast images of salivary glands. All animals are stage 16 $sinu^{nwu7}$/+ heterozygotes (WT) or $sinu^{nwu7}$ homozygotes (*sinu*). To allow comparison between images stained for a given marker, heterozygous and homozygous embryos were imaged on the same slide using the same confocal settings, and all image adjustments were applied equally to resulting images. Bars: B′, 5 μm (for A′ and B′); D′, 15 μm (for C–D′); B′′′, 5 μm (for all other images).

sential for septa formation, Sinuous has a critical role in attaining the correct number of septa and in organizing septa into contiguous circumferential ribbons.

Sinuous does not appear to be required for adherens junction organization or overall cell polarity, as the adherens junctions in *sinuous* mutants have normal ultrastructure by TEM and septa remain localized to the apical half of the lateral plasma membrane (Fig. 5 B; unpublished data). These results are consistent with the normal localization and appearance of the adherens junctions markers Arm and DE-cadherin and the apical marker Dlt by confocal microscopy (Fig. 4, K–L′′; unpublished data). However, TEM reveals that tracheal cells (but not epidermal or salivary gland cells) had ultrastructural defects in addition to the disruption of septate junctions. Tracheal cells secrete a specialized highly patterned cuticle, the taenidium, that normally forms a rigid spiral that lines the tracheal lumen. Cross sections of the taenidium in wild-type animals show a regular sequence of cuticle ridges separated by valleys (Fig. 5 F). In contrast, the taenidium in *sinuous* mutants displays a highly irregular folding pattern (Fig. 5 G). In addition, tracheal cells (but not the epidermal or salivary gland cells) in stage 17 *sinuous* mutants stain poorly with tuloudine blue/methylene blue compared with wild-type tracheal cells and other cells in *sinuous* mutants (Fig. 5, D and E; unpublished data). Ultrastructurally, this staining abnormality correlated with the presence of an unusually large number of vesicles in the cytoplasm of *sinuous* mutant tracheal cells, an apparent increased cell volume and a lower density of ribosome-rich cytoplasmic matrix (Fig. 5 G). Although the significance of the cytoplasmic architecture defects in *sinuous* mu-

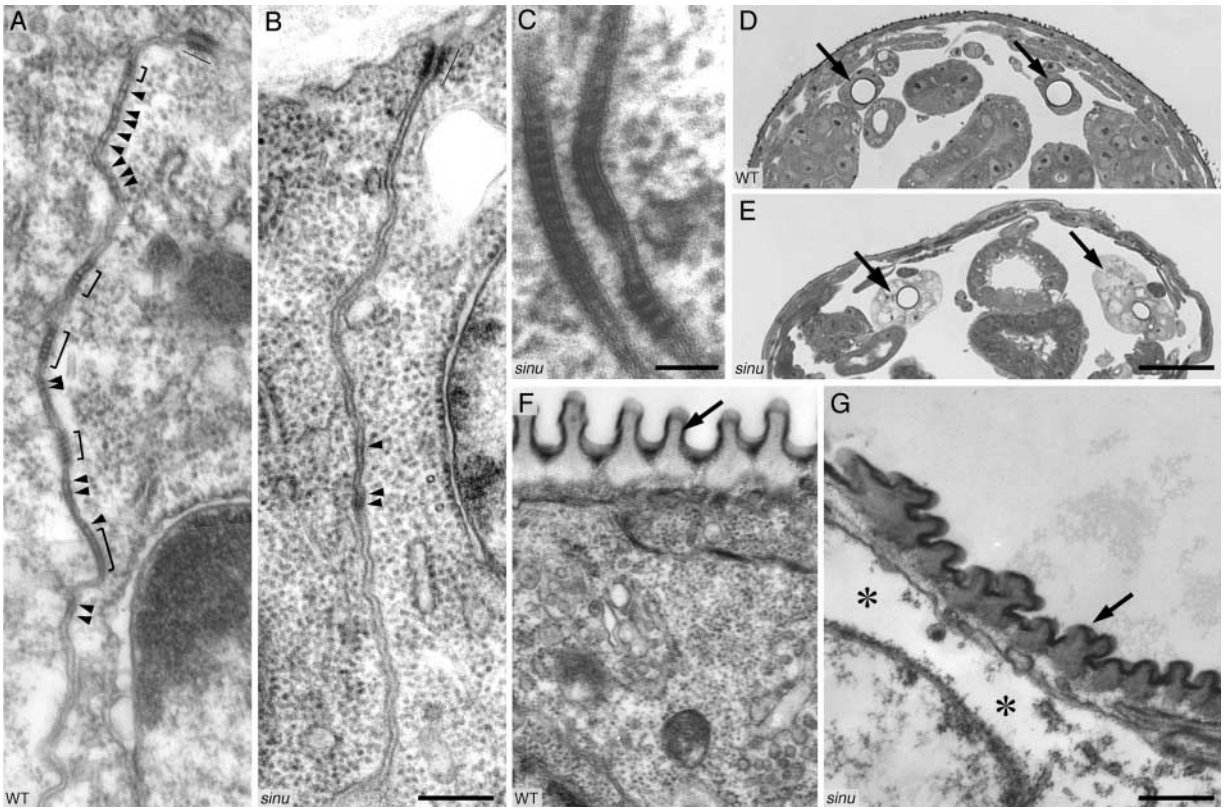

Figure 5. **Sinuous is required for septate junction organization, but not for septa formation.** (A) TEM of late stage 17 wild-type epidermis showing the zonula adherens (thin line) and septate junctions. Brackets indicate clustered groups of septa, and arrowheads point to individual septa. (B and C) TEM of late stage 17 *sinuous* mutant epidermis. In some sections, such as the one shown in B, septa are absent except for some poorly differentiated intercellular material (arrowheads) at cell–cell contacts. However, in other sections, such as the one shown in C, cell–cell contacts display normally organized septate junctions. The zonula adherens (B, thin line) appears normal in *sinuous* mutants. (D and E) Toluidine blue/methylene blue–stained cross sections of a stage 17 wild-type (D) and a *sinuous* mutant (E) embryo. Arrows point to the tracheal dorsal trunks. Note that the staining intensity of *sinuous* mutant tracheal cells is lighter and that the cell shape is more cuboidal than in the wild-type, whereas the epidermis in *sinuous* mutants stains similarly to wild-type epidermis. (F and G) TEM of dorsal tracheal trunks of late stage 17 wild-type (F) and *sinuous* mutant (G) embryos. In *sinuous* mutants, the taenidium (arrows) shows an irregular morphology, and the cytoplasm has large empty spaces (asterisks). Genotypes: WT, Oregon-R; $sinu^{nwu7}$. Bars: B, 200 nm (for A and B); C, 50 nm; E, 25 μm (for D and E); G, 300 nm (for F and G).

tants is unclear, the cuticular defects are consistent with previous results showing the septate junction genes *cor* and *nrx* are required for normal apical cuticle morphogenesis (Fehon et al., 1994; Baumgartner et al., 1996).

Sinuous localization depends on other septate junction components

Because the above confocal and TEM results show that Sinuous is required for septate junction organization, we asked whether Sinuous localization depended on other septate junction components or whether Sinuous might nucleate septate junction formation by localizing other proteins to the septate junction. In *cor*, *nrx*, *mega*, and *nrv2* null mutants, Sinuous was mislocalized laterally in the trachea, hindgut, salivary glands, and epidermis (Fig. 3, E–H′′; unpublished data). Thus, the localization of Sinuous depends on other septate junction components.

Sinuous acts in one branch of a tube size control pathway

To further define the function of Sinuous in tracheal tube size control, we investigated the relationship between *sinuous* and other tracheal tube expansion genes using double-mutant analysis. To interpret double-mutant phenotypes, we first determined that Sinuous does not appear to have a maternal contribution because staining *sinuous* zygotic null embryos with the anti-Sinuous antibody did not reveal any detectable Sinuous expression at any stage (Fig. S2; unpublished data). Next, we analyzed the phenotypes of double-mutant combinations of a *sinuous* null mutant and mutations in other genes known to be required for tracheal tube expansion (Beitel and Krasnow, 2000; Paul et al., 2003). Trachea in *sinu nrx* double-null mutants have the same phenotypes as either null single mutant (Fig. 6 D), consistent with *sinuous* and *nrx* having the same genetic function in tracheal tube size control and acting in a single linear pathway. In contrast, the combinations of a *sinuous* null mutation and mutations in *nrv2* or the uncloned genes *vari*, *conv*, and *cystic* cause moderately to dramatically more severe tube size defects than the *sinuous* null mutation alone, indicating that *sinuous* does not have the identical genetic function as these genes in tracheal tube size control (Fig. 6, F–L; unpublished data). In particular, compared with either *sinuous* or *nrv2* null mutants, *nrv2*;*sinu* double null mutants have somewhat more severe diameter expansions that are most evident in the

transverse connectives, and numerous spherical cyst-like structures in the lateral trunks and ganglionic branches (Fig. 6, F and H). The *vari*;*sinu* and *conv*;*sinu* double mutants both have severe diameter defects in all multicellular branches, and dorsal trunk length appears to be increased (Fig. 6, J and L), but the *conv*;*sinu* double is more severe than the *vari*;*sinu* double in that by stage 16, most tracheal branches fail to stain for the 2A12 lumenal antigen (Fig. 6 L). The *cystic*;*sinu* double mutant is so severe that by stage 16, only a few cyst-like structures were visible by 2A12 staining and the remainder of the tracheal system was not visible by differential interference contrast optics (unpublished data). Together, these results suggest that *sinuous* and *nrx* have a genetic function in tracheal tube size control that is distinguishable from the functions of *nrv2*, *vari*, *conv*, and *cystic*.

We also found that *sinuous* interacts with *scrib*, a septate junction gene that has not previously been shown to have a role in tracheal tube size control (Bilder and Perrimon, 2000). The tracheal dorsal trunks of animals heterozygous for both *scrib* and *sinuous* mutations become abnormally long during stage 17 (unpublished data). This interaction is unusual because transheterozygous combinations of *sinuous* with either *nrx*, *nrv2*, *cor*, *conv*, *vari*, or *cystic* do not cause tracheal defects (unpublished data) and suggests that *sinuous* and *scrib* may act in the same genetic pathway. This possibility is supported by *sinuous scrib* double homozygotes having the same phenotype as the single *sinuous* null mutants (Fig. 6 M). Thus, *sinuous, nrx, and scrib* appear to define a branch of the tracheal tube size control pathway that is distinguishable from the pathways in which *nrv2*, *cystic*, *vari*, and *conv* act.

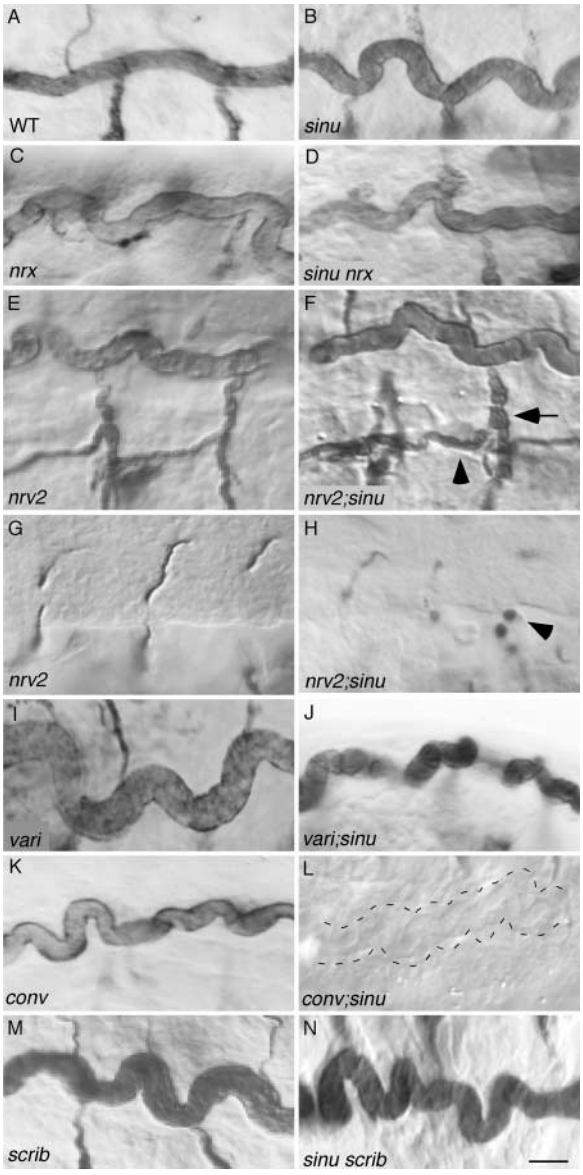

Figure 6. **Sinuous acts in one branch of a tube size control pathway.** *sinu nrx* (D) and *sinu scrib* (N) double mutants have the same phenotype as *sinu* single mutants (B), suggesting that *scrib* and *nrx* act in the same genetic pathway as *sinuous*. In contrast, double mutant combinations of a *sinuous* null mutation with *nrv2*, *conv* or *vari*, mutations (F, H, J, and L) all cause tracheal phenotypes that are more severe than the *sinuous* null mutation (B), suggesting that these genes act in a genetic pathway(s) or branch of a pathway(s) that *sinuous* does not act in. *nrv2*;*sinu* double mutants have somewhat more severe diameter expansions in the transverse connective and visceral branches (F, arrow and arrowhead, respectively) and have cyst-like structures (H, arrowhead) in their ganglionic branches compared with *sinuous* or *nrv2* null mutants (compare Fig. 6 H to Fig. 1 I). *conv*;*sinu* double mutants have greatly increased length and diameter defects in all multicellular branches, and the dorsal trunk fails to stain with the lumenal antigen 2A12 by mid-stage 16 (L, dotted lines outline the dorsal trunk). Genotypes: WT, Oregon-R; $sinu^{nwu7}$; nrx^{4865}; *nrv2*, $nrv2^{23B}$ in E, $nrv2^{nwu3}$ in G; $conv^{J(2)k06507}$; $var^{jl(2)03953}$; *scrib*, $scrib^{2}$/ $scrib^{j7B3}$ in M, $scrib^{2}$ in N. Bar in N (represents all panels), 5 μm.

Discussion

An evolutionarily conserved role for claudins in barrier junction function

We have cloned the gene *sinuous* and found that it encodes a protein that is molecularly and functionally similar to vertebrate claudins. Sinuous has all of the amino acids absolutely conserved across vertebrate claudins and has as much sequence similarity to canonical vertebrate claudins as do some of the more divergent vertebrate claudins. Sinuous also has functional similarity to vertebrate claudins because it localizes to and is required for the function of paracellular barrier junctions. Thus, by multiple criteria, Sinuous can be considered a claudin.

Our finding that a *Drosophila* claudin is required for paracellular barrier function is significant because there has been minimal evidence of a conserved molecular basis for the barrier functions of invertebrate septate junctions and vertebrate tight junctions. In combination with the recent finding that *C. elegans* paracellular barrier function also requires claudins (Asano et al., 2003), our results raise the possibility that the different types of barrier junctions present in diverse species evolved from a common ancestral claudin-containing barrier junction. They also raise the possibility that vertebrate paranodal junctions (for review see Tepass et al., 2001), which have significant morphological, functional, and molecular similarities to septate junctions, may also contain claudins.

If paracellular barrier junctions all evolved from a common ancestor, there currently exists a remarkable number of differences between the subcellular localization, ultrastructure, and molecular composition of these junctions. For example, as detailed in the introduction, tight junctions are

apical to the adherens junction, whereas septate junctions are basal. Tight junctions have a series of "kissing points," septate junctions have ladder-like septa, and *C. elegans* barrier junctions have neither kissing points nor ladder-like septa (Asano et al., 2003). One explanation for this variability may lie in the multiple distinct nonbarrier functions of these junctions. Although claudins are essential for barrier function, junctional morphology and localization may be dictated by components whose cellular functions, such as cell polarization, signaling, or directed secretion, are not directly involved in paracellular barrier formation. Thus, rather than trying to describe entire junctional complexes as being analogous or homologous, it may be more useful to define and compare aspects of these junctions in terms of particular functions and protein components.

Sinuous is required for septate junction organization, but not for septa formation

In *sinuous* mutants, septate junction organization is disrupted at both the confocal and TEM levels. In all tissues examined, the number of septa is reduced and there are cell–cell contacts devoid of septa. Thus, Sinuous is required for normal septate junction organization. Surprisingly, in contrast to Nrx, Cor, Nrv2, Dlg, and Mega (Baumgartner et al., 1996; Lamb et al., 1998; Behr et al., 2003; Bilder et al., 2003; Genova and Fehon, 2003), Sinuous is not absolutely required for septa formation. This is reminiscent of the role of Gliotactin, which is required for ribbon organization, but not septa formation (Schulte et al., 2003). However, in contrast to Gliotactin, the number of septa is reduced in *sinuous* mutants, indicating that Sinuous is required for both organization and formation on the normal number of septa. The ability of morphologically normal septa to form in the absence of Sinuous may result from septate junctions containing at least one other *Drosophila* claudin and at least five other transmembrane proteins (Baumgartner et al., 1996; Behr et al., 2003; Genova and Fehon, 2003; Paul et al., 2003; Schulte et al., 2003). Whether the remaining septa in *sinuous* mutants have normal barrier function is an interesting but difficult to answer question, as the discontinuities in the septal ribbons breach the paracellular diffusion barrier and obscure the barrier properties of remaining septa.

Sinuous function in epithelial tube size control

An additional function of Sinuous that appears to be distinct from its role in barrier formation is that Sinuous is required for tracheal tube size control. The disruption of paracellular barriers in *sinuous* mutants is unlikely to be the cause of tracheal tube size defects, as we have previously shown that mutations in different genes cause qualitatively different tracheal tube size defects despite causing equivalent barrier defects (Paul et al., 2003). For example, *cystic* mutants have severe diameter but no length defects, whereas *mega* mutants have length but almost no diameter defects. In addition, mutants can have barrier defects but minimal tracheal size defects (Paul et al., 2003).

Our present results extend the distinction between barrier and tube size functions by showing that the presence or absence of septa, which are thought to form the paracellular barrier, are not correlated with tracheal tube size defects. Specifically, although *sinuous* and *nrx* mutants have the same tracheal phenotypes, well-differentiated septa are present in *sinuous* but not *nrx* mutants. Furthermore, although septa are presumably absent in *nrx sinu* double mutants, an *nrx* null mutation does not enhance the *sinuous* null mutant phenotype. In contrast, mutations in the genes *cystic* and *vari,* which cause septate junction barrier defects (Paul et al., 2003), strongly enhance the phenotypes of both *sinuous* null mutants, which have septa, and of *nrv2* null mutants, which have few or no septa (Genova and Fehon, 2003; compare Fig. 6 J in this paper with Fig. 5 L in Paul et al., 2003). These observations imply that there are molecular complexes that control tracheal tube size that do not correspond to the septa visible by TEM. Although additional work is required to define the molecular composition and function of the septate junction–associated complexes that mediate tracheal tube size control, the conservation of the proteins that function in tracheal tube size control suggests that this mechanism of tube size control may also be conserved.

The *Drosophila* claudins Sinuous and Mega have distinct functions

Behr et al. (2003) recently reported that *mega* also encodes a *Drosophila* claudin, providing an opportunity to compare the in vivo functions of two claudins required for barrier formation in the same tissues. The lengths of multicellular tracheal tubes are increased in both *mega* and *sinuous* mutants, but the effects of *sinuous* and *mega* mutations on cellular and junctional architecture are very different. In *sinuous* mutants, morphologically normal but discontinuous septa are present, and apical cuticle patterning is abnormal. By contrast, in *mega* mutants, apical surface patterning appears normal, but no septa form, and instead unstructured intercellular material is seen (Behr et al., 2003). Overexpression of Mega (but not Sinuous) can mislocalize Cor and Nrx (Behr et al., 2003; unpublished data). Thus, although Sinuous and Mega may be partially redundant, they have different functions in septate junction formation. As the exact roles of claudins in formation and organization of tight junctions and septate junctions have not yet been fully determined, the molecular-genetic tools available in *Drosophila* coupled with the limited number of *Drosophila* claudins provide an excellent opportunity for understanding the multiple functions of claudins in barrier junction formation and function.

Materials and methods

Fly stocks, genetics, and mutations

Fly stocks were obtained from the Bloomington *Drosophila* Stock Center (Indiana University Bloomington, Bloomington, IN) or from published sources. *sinu*^{nwu7} was generated by imprecise excision of the l(3)06524 transposable element, and the sequence across the break point is 5′-acggtgggccttttt/aagtcagggtcggtc-3′. For the dye exclusion assay, Texas red–labeled 10-kD dextran (Molecular Probes, Inc.) was injected into the hemocoel of late stage 16 homozygous embryos as described by Lamb et al. (1998) using a TM3 Actin-GFP balancer chromosome to identify homozygous versus heterozygous embryos.

Immunofluorescence

Primary antibodies and dilutions were used as follows: anti-tracheal lumen 2A12 and anti-Arm N27A1 1:100 (Developmental Studies Hybridoma Bank [DSHB]), mouse anti-Cor C566.9^{C} and C615.16^{B} 1:500 and guinea pig anti-Cor 1:10,000, respectively (a gift from R. Fehon, Duke

University, Durham, NC), anti-E-cadherin DECAD2 1:20 (Oda et al., 1994), anti-FasIII 7G10 1:50 (DSHB), anti-Dlg 1:500 (Woods et al., 1997), anti-Dlt 1:200 (Bhat et al., 1999), anti-Na/K ATPase α-subunit α5 1:50 (DSHB), and anti-Nrx 1:200 (Baumgartner et al., 1996). Rabbit anti-Sinuous sera was generated against the peptide NH_2-CSEAHVQH-KKRIQFKESQTRFELVRG-CO_2H conjugated to keyhole limpet hemocyanin via the NH_2-terminal cysteine (Harlan Bioproducts for Science, Inc.) and used at 1:2,000 without purification. The specificity of the anti-Sinuous antibody was established by determining that the antisera did not visibly stain animals homozygous for the *sinu*^{nwu7} null mutation (Fig. S2, available at http://www.jcb.org/cgi/content/full/jcb.200309134/DC1). Embryos for Arm and Sinuous staining were heat fixed and processed as previously described (Miller et al., 1989; Samakovlis et al., 1996). Embryos for Na/K ATPase staining were fixed in 4% PFA and hand devitellinized. All other fixation and staining was performed as described previously (Samakovlis et al., 1996). Secondary antibodies conjugated to Cy5 (Jackson ImmunoResearch Laboratories) or Alexa® 546 (Molecular Probes, Inc.) were used at 1:200. Confocal images were acquired on a confocal laser scanning microscope (model TCS SP2; Leica). To estimate relative levels of staining, heterozygous and homozygous embryos were imaged on the same slide in the same session. Photomultiplier tube and laser levels were adjusted to just saturate heterozygous images, and homozygous embryos were then imaged at the same levels. Images were processed using Adobe Photoshop®. Level adjustments were applied equally to matched heterozygous and homozygous images.

Electron microscopy

Late stage 17 embryos were injected with 5% glutaraldehyde in 100 mM phosphate buffer (pH 7.2; Prokop et al., 1998). Embryos were then covered with 2.5% glutaraldehyde in 100 mM phosphate buffer (pH 7.2), and the anterior and posterior tips were cut off. After 30 min in fixative, embryos were collected in an eppendorf tube, osmicated for 1 h, and en bloc contrasted with uranyl acetate for 30 min. After dehydration, embryos were embedded in Epon/Araldite, and ultrathin sections were examined on a transmission electron microscope (model H-7100; Hitachi). Negatives were scanned and imported into Adobe Photoshop® 7.0 for image assembly. Counts are expressed as the average ± SEM.

Molecular biology

Inverse PCR was performed according to the protocol of the Berkeley Drosophila Genome Project (BDGP, University of California, Berkeley, Berkeley, CA; http://www.fruitfly.org/about/methods/inverse.pcr.html). The sequences flanking the insertion were 5′-gtttgcaacgcccag/ttggtcagtgattac-3′.

The *sinuous* cDNA LD29359 was obtained from the BDGP and a second cDNA, WuP1, was obtained though a cDNA library screen of the BDGP P1 library. The complete sequence of both cDNAs was determined using BigDye® sequencing (Applied Biosystems), which revealed that the LD29359 cDNA had been spliced at a non-GT site and would encode a protein with a different COOH terminus than the WuP1 cDNA. Because nine additional cDNAs obtained from the BDGP all had the WuP1 splice site, it appears that LD29359 is either a rare alternative splice form or the product of an aberrant splicing reaction. We also noted that in the genomic DNA sequence, the 5′ end of the *sinuous* ORF extended beyond the beginning of both the LD29359 and WuP1 cDNAs, and that the predicted Sinuous NH_2 terminus was unusually long for a claudin (38 vs. <10 aa). However, the similar start site of all 11 *sinuous* cDNAs and the single band of the correct sequence obtained in 5′ RACE experiments (First Choice RLM Race kit; Ambion) indicated that the correct 5′ end of the *sinuous* transcription unit had been identified. This conclusion was further supported by the conservation of the predicted long NH_2 terminus, but not the extended 5′ genomic ORF, in *the sinuous* homologue we identified in the genome of *Drosophila psuedoobscura*. The UAS-Sinuous transgene was constructed by inserting the WuP1 cDNA into the pUAST vector and creating transgenic flies (Brand and Perrimon, 1993).

RNA interference experiments were performed by PCR amplifying the *sinuous* ORF using primers containing T7 promoter sites (5′-taatacgactcactatagggagaccaaaaccagcgaaattccaatag-3′ and 5′-taatacgactcactatagggagaccacagggttaacacagtacccaca-3′), in vitro transcription, and injection of double-stranded RNA into early *btl*-Gal4 UAS GFP embryos according to the method of Kennerdell and Carthew (1998). Embryos were allowed to develop to stage 16–17 and were examined by epifluorescence using a I microscope (Axioplan I; Carl Zeiss MicroImaging, Inc.).

The GenBank/EMBL/DDBJ accession nos. of the sequences analyzed in this paper are as follows: LD29359, AY069562; WuP1, AY423544; RE71866, CF674931; RE28927, CF674930; RE13637, CF674932; RE12528, CF674933; RE33979, CF674929; RE48192, CF674935; RE71666, CF674934; RE06244, CF674938; RE70362, CF674936; and RE68393, CF674937.

Sequence comparisons and phylogenetic analyses

ClustalW and phylogenetic tree analyses were performed using the MacVector program (Accelrys) using the relatively more conserved sequences from the region spanning the beginning of the first through the end of the fourth transmembrane domains predicted by TMHMM for each claudin family member. The number of conserved residues between chordate claudins and any particular invertebrate claudin family member was determined by using ClustalW to align the 36 claudins studied by Kollmar et al. (2001) and a given invertebrate claudin family member. No manual editing of the aligned sequences was performed, with the exception that the residues of the *C. elegans* CLC genes in the region of the "GLW" motif were adjusted to match the alignment of Asano et al. (2003). However, we note that in alignments containing larger numbers of invertebrate claudins that an RGF sequence in Sinuous aligns with the RAL motif present in most chordate claudins, and would give Sinuous 10 rather than 9 of 13 conserved amino acids (potentially conserved R underlined). The aligned sequences of the claudins used for Fig. 2 are shown in Fig. S1. The phylogenetic tree in Fig. 2 was generated from 1,000 bootstrap repetitions using the neighbor joining method, gap site ignored, random tie breaking of branches with equal values, and an uncorrected "p."

Online supplemental material

Fig. S1 shows the alignment of the set of claudin family members used to generate the phylogenetic tree in Fig. 2. The alignment was generated as described above. The 13 residues conserved among 90% of the human, zebrafish, and urochordate claudins analyzed by Kollmar et al. (2001) are shown below the alignment. Fig. S2 (A) shows the specificity of the anti-Sinuous antibody, and lack of maternally derived or provided Sinuous protein is demonstrated by the strong staining of animals heterozygous (but not homozygous) for the *sinu*^{nwu7} null mutation. Stage 16 embryos are shown. Fig. S2 (B–D′′′) shows expression and subcellular localization of Sinuous. Sinuous (B and C, red) predominantly localizes to the septate junction region marked by Cor (B and D, green) in the hindgut and other ectodermal tissues at stages 13/14, and 14 (B–D; B′–D′). At stages 15 and 16, Sinuous almost entirely colocalizes with Cor at the septate junction (B′′–D′′; B′′′–D′′′). Dotted lines outline basal cell surfaces. Online supplemental material is available at http://www.jcb.org/cgi/content/full/jcb.200309134/DC1.

We thank the Holgmren and Carthew labs for assistance; Rich Carthew and Sarah Paul for comments on the manuscript; M. Yu for RNAi; W. Russin of the Northwestern Biological Imaging Facility for imaging advice; and Jason Rosenbaum and Iswar Radhakrishnan for help on bioinformatics and phylogeny.

We thank Henry Hong for technical assistance with the TEM work, which was supported by a Premiers Excellence Research Award, and grants from the National Science and Research Council of Canada and the Canadian Institute of Health Research to U. Tepass. V.M. Wu was supported by the National Institutes of Health Cellular and Molecular Basis of Disease training grant #T32 GM008061, and G.J. Beitel is a recipient of a Burroughs Welcome Fund Career Award in the Biomedical Sciences (10015885).

Submitted: 23 September 2003
Accepted: 25 November 2003

References

Anderson, J.M. 2001. Molecular structure of tight junctions and their role in epithelial transport. *News Physiol. Sci.* 16:126–130.

Asano, A., K. Asano, H. Sasaki, M. Furuse, and S. Tsukita. 2003. Claudins in *Caenorhabditis elegans*: their distribution and barrier function in the epithelium. *Curr. Biol.* 13:1042–1046.

Bateman, A., E. Birney, L. Cerruti, R. Durbin, L. Etwiller, S.R. Eddy, S. Griffiths-Jones, K.L. Howe, M. Marshall, and E.L.L. Sonnhammer. 2002. The Pfam protein families database. *Nucleic Acids Res.* 30:276–280.

Baumgartner, S., J.T. Littleton, K. Broadie, M.A. Bhat, R. Harbecke, J.A. Lengyel, R. Chiquet-Ehrismann, A. Prokop, and H.J. Bellen. 1996. A *Drosophila* neurexin is required for septate junction and blood-nerve barrier formation and function. *Cell.* 87:1059–1068.

Behr, M., D. Riedel, and R. Schuh. 2003. The claudin-like megatrachea is essential

in septate junctions for the epithelial barrier function in *Drosophila*. *Dev. Cell.* 5:611–620.

Beitel, G.J., and M.A. Krasnow. 2000. Genetic control of epithelial tube size in the *Drosophila* tracheal system. *Development.* 127:3271–3282.

Bhat, M.A., S. Izaddoost, Y. Lu, K.O. Cho, K.W. Choi, and H.J. Bellen. 1999. Discs Lost, a novel multi-PDZ domain protein, establishes and maintains epithelial polarity. *Cell.* 96:833–845.

Bilder, D., and N. Perrimon. 2000. Localization of apical epithelial determinants by the basolateral PDZ protein Scribble. *Nature.* 403:676–680.

Bilder, D., M. Schober, and N. Perrimon. 2003. Integrated activity of PDZ protein complexes regulates epithelial polarity. *Nat. Cell Biol.* 5:53–58.

Brand, A.H., and N. Perrimon. 1993. Targeted gene expression as a means of altering cell fates and generating dominant phenotypes. *Development.* 118: 401–415.

Christophe-Hobertus, C., C. Szpirer, R. Guyon, and D. Christophe. 2001. Identification of the gene encoding brain cell membrane protein 1 (BCMP1), a putative four-transmembrane protein distantly related to the peripheral myelin protein 22/epithelial membrane proteins and the claudins. *BMC Genomics.* 2:3.

Claude, P., and D.A. Goodenough. 1973. Fracture faces of zonulae occludentes from "tight" and "leaky" epithelia. *J. Cell Biol.* 58:390–400.

Colegio, O.R., C.M. Van Itallie, H.J. McCrea, C. Rahner, and J.M. Anderson. 2002. Claudins create charge-selective channels in the paracellular pathway between epithelial cells. *Am. J. Physiol. Cell Physiol.* 283:C142–C147.

Colegio, O.R., C. Van Itallie, C. Rahner, and J.M. Anderson. 2003. Claudin extracellular domains determine paracellular charge selectivity and resistance but not tight junction fibril architecture. *Am. J. Physiol. Cell Physiol.* 284: C1346–C1354.

Farquhar, M., and G. Palade. 1963. Junctional complexes in various epithelia. *J. Cell Biol.* 17:375–412.

Fehon, R.G., I.A. Dawson, and S. Artavanis-Tsakonas. 1994. A *Drosophila* homologue of membrane-skeleton protein 4.1 is associated with septate junctions and is encoded by the *coracle* gene. *Development*. 120:545–557.

Fristrom, D.K. 1982. Septate junctions in imaginal disks of *Drosophila*: a model for the redistribution of septa during cell rearrangement. *J. Cell Biol.* 94:77–87.

Furuse, M., H. Sasaki, K. Fujimoto, and S. Tsukita. 1998. A single gene product, claudin-1 or -2, reconstitutes tight junction strands and recruits occludin in fibroblasts. *J. Cell Biol.* 143:391–401.

Furuse, M., M. Hata, K. Furuse, Y. Yoshida, A. Haratake, Y. Sugitani, T. Noda, A. Kubo, and S. Tsukita. 2002. Claudin-based tight junctions are crucial for the mammalian epidermal barrier: a lesson from claudin-1-deficient mice. *J. Cell Biol.* 156:1099–1111.

Genova, J.L., and R.G. Fehon. 2003. Neuroglian, Gliotactin, and the Na^+/K^+ ATPase are essential for septate junction function in *Drosophila*. *J. Cell Biol.* 161: 979–989.

Kennerdell, J.R., and R.W. Carthew. 1998. Use of dsRNA-mediated genetic interference to demonstrate that frizzled and frizzled 2 act in the wingless pathway. *Cell.* 95:1017–1026.

Knust, E., and O. Bossinger. 2002. Composition and formation of intercellular junctions in epithelial cells. *Science.* 298:1955–1959.

Kollmar, R., S.K. Nakamura, J.A. Kappler, and A.J. Hudspeth. 2001. Expression and phylogeny of claudins in vertebrate primordia. *Proc. Natl. Acad. Sci. USA.* 98:10196–10201.

Kubota, K., M. Furuse, H. Sasaki, N. Sonoda, K. Fujita, A. Nagafuchi, and S. Tsukita. 1999. Ca^{2+}-independent cell-adhesion activity of claudins, a family of integral membrane proteins localized at tight junctions. *Curr. Biol.* 9:1035–1038.

Lamb, R.S., R.E. Ward, L. Schweizer, and R.G. Fehon. 1998. *Drosophila* coracle, a member of the protein 4.1 superfamily, has essential structural functions in the septate junctions and developmental functions in embryonic and adult epithelial cells. *Mol. Biol. Cell.* 9:3505–3519.

Lane, N.J., and L.S. Swales. 1982. Stages in the assembly of pleated and smooth septate junctions in developing insect embryos. *J. Cell Sci.* 56:245–262.

Manning, G., and M.A. Krasnow. 1993. Development of the *Drosophila* tracheal system. *In* The Development of *Drosophila melanogaster*. Vol. 1. M. Bate and A. Martinez-Arias, editor. Cold Spring Harbor Laboratory Press, Cold Spring Harbor, NY. 609–685.

Miller, K.G., C.M. Field, and B.M. Alberts. 1989. Actin-binding proteins from *Drosophila* embryos: a complex network of interacting proteins detected by F-actin affinity chromatography. *J. Cell Biol.* 109:2963–2975.

Morita, K., M. Furuse, K. Fujimoto, and S. Tsukita. 1999. Claudin multigene family encoding four-transmembrane domain protein components of tight junction strands. *Proc. Natl. Acad. Sci. USA.* 96:511–516.

Nitta, T., M. Hata, S. Gotoh, Y. Seo, H. Sasaki, N. Hashimoto, M. Furuse, and S. Tsukita. 2003. Size-selective loosening of the blood-brain barrier in claudin-5-deficient mice. *J. Cell Biol.* 161:653–660.

Oda, H., T. Uemura, Y. Harada, Y. Iwai, and M. Takeichi. 1994. A *Drosophila* homolog of cadherin associated with armadillo and essential for embryonic cell-cell adhesion. *Dev. Biol.* 165:716–726.

Paul, S.M., M. Ternet, P.M. Salvaterra, and G.J. Beitel. 2003. The Na^+/K^+ ATPase is required for septate junction function and epithelial tube-size control in the *Drosophila* tracheal system. *Development*. 130:4963–4974.

Prokop, A., J. Uhler, J. Roote, and M. Bate. 1998. The kakapo mutation affects terminal arborization and central dendritic sprouting of *Drosophila* motorneurons. *J. Cell Biol.* 143:1283–1294.

Samakovlis, C., G. Manning, P. Steneberg, N. Hacohen, R. Cantera, and M.A. Krasnow. 1996. Genetic control of epithelial tube fusion during *Drosophila* tracheal development. *Development.* 122:3531–3536.

Schneeberger, E.E., and R.D. Lynch. 1992. Structure, function, and regulation of cellular tight junctions. *Am. J. Physiol. Cell Physiol.* 262:L647–L661.

Schulte, J., U. Tepass, and V.J. Auld. 2003. Gliotactin, a novel marker of tricellular junctions, is necessary for septate junction development in *Drosophila*. *J. Cell Biol.* 161:991–1000.

Simske, J.S., M. Koppen, P. Sims, J. Hodgkin, A. Yonkof, and J. Hardin. 2003. The cell junction protein VAB-9 regulates adhesion and epidermal morphology in *C. elegans*. *Nat. Cell Biol.* 5:619–625.

Sonnhammer, E.L., G. von Heijne, and A. Krogh. 1998. A hidden Markov model for predicting transmembrane helices in protein sequences. *Proc. Int. Conf. Intell. Syst. Mol. Biol.* 6:175–182.

Staehelin, L.A. 1974. Structure and function of intercellular junctions. *Int. Rev. Cytol.* 39:191–282.

Tepass, U., and V. Hartenstein. 1994. The development of cellular junctions in the *Drosophila* embryo. *Dev. Biol.* 161:563–596.

Tepass, U., G. Tanentzapf, R. Ward, and R. Fehon. 2001. Epithelial cell polarity and cell junctions in *Drosophila*. *Annu. Rev. Genet.* 35:747–784.

Tsukita, S., and M. Furuse. 2002. Claudin-based barrier in simple and stratified cellular sheets. *Curr. Opin. Cell Biol.* 14:531–536.

Tsukita, S., M. Furuse, and M. Itoh. 2001. Multifunctional strands in tight junctions. *Nat. Rev. Mol. Cell Biol.* 2:285–293.

Woods, D.F., J.W. Wu, and P.J. Bryant. 1997. Localization of proteins to the apico-lateral junctions of *Drosophila* epithelia. *Dev. Genet.* 20:111–118.